Implications of temperature variation for malaria parasite development across Africa

J. I. Blanford[1], S. Blanford[2], R. G. Crane[3], M. E. Mann[4], K. P. Paaijmans[2], K. V. Schreiber[5] & M. B. Thomas[2]

[1]GeoVISTA Center, Department of Geography, The Pennsylvania State University, University Park, PA, USA, [2]Center for Infectious Disease Dynamics and Department of Entomology, Merkle Lab, The Pennsylvania State University, University Park, PA, USA, [3]AESEDA, Department of Geography, The Pennsylvania State University, University Park, PA, USA, [4]Department of Meteorology, and Earth and Environmental Systems Institute, The Pennsylvania State University, University Park, PA, USA, [5]Department of Geography, Millersville University of Pennsylvania, Millersville, PA, USA.

Temperature is an important determinant of malaria transmission. Recent work has shown that mosquito and parasite biology are influenced not only by average temperature, but also by the extent of the daily temperature variation. Here we examine how parasite development within the mosquito (Extrinsic Incubation Period (EIP)) is expected to vary over time and space depending on the diurnal temperature range and baseline mean temperature in Kenya and across Africa. Our results show that under cool conditions, the typical approach of using mean monthly temperatures alone to characterize the transmission environment will underestimate parasite development. In contrast, under warmer conditions, the use of mean temperatures will overestimate development. Qualitatively similar patterns hold using both outdoor and indoor temperatures. These findings have important implications for defining malaria risk. Furthermore, understanding the influence of daily temperature dynamics could provide new insights into ectotherm ecology both now and in response to future climate change.

C limate plays an important role in the dynamics and distribution of malaria[1–7]. Although rainfall is critical in providing suitable habitats for mosquitoes to breed[3,8,9], temperature is a key driver of several of the essential mosquito and parasite life history traits that combine to determine transmission intensity, including mosquito development rate, biting rate, and development rate and survival of the parasite within the mosquito (see Ref. 10). Accordingly, a number of studies have used environmental temperature (sometimes together with rainfall and/or humidity) to develop maps representing spatial and/or temporal variation in malaria transmission risk (e.g. Refs. 3,5,11–13).

A common feature of such studies is the characterization of environmental conditions using relatively coarse aggregate measures such as mean monthly temperatures. Recently, however, Paaijmans *et al.*[14,15] demonstrated that malaria mosquito and parasite biology are influenced not only by average temperature, but also by the extent of the temperature variation that occurs throughout the day (see also Lambrechts, et al.[16] for analogous effects with dengue). The effects, which appear to derive at least in part from non-linear rate summation (Jensen's inequality – see Refs. 17,18), lead to different influences of daily temperature dynamics depending on where the baseline mean temperature sits on the thermal performance curve of a particular trait. In general, daily fluctuation around cooler temperatures acts to speed up rate processes relative to the mean, fluctuation around warmer temperatures acts to slow them down, and fluctuation around intermediate temperatures tends to have little net effect[14,15]. Thus, while use of mean temperatures might be appropriate under certain conditions, we expect in general that use of mean temperatures will either over or underestimate individual traits and hence, composite metrics of transmission intensity such as vectorial capacity or the basic reproductive rate (R_0).

Here we examine how parasite development is expected to vary over time and space depending on the extent of diurnal temperature range and baseline mean temperature. We focus on parasite development as defined by the Extrinsic Incubation Period, or EIP, which describes the length of time it takes for a parasite to complete development within the mosquito from initial acquisition via an infected blood meal to the point at which it can be transmitted to another host via a further blood meal. The EIP is one of the most influential para-meters determining malaria transmission intensity[19,20]. In addition, the EIP is known to be very sensitive to temperature and to vary non-linearly such that small changes in temperature can have potentially large effects on

transmission[1,15,21]. We begin by examining four sites in Kenya using detailed temperature records to compare estimates of EIP based on measures of mean temperature vs. the hourly fluctuating temperatures experienced in the field. Utilizing these site-specific insights, we then scale up to explore the influence of daily temperature variation on EIP across the malaria transmission range within Kenya, and then Africa. Consistent with expectations, we find contrasting effects of daily temperature dynamics across time and space, with both increases and decreases in parasite development relative to standard predictions based on mean temperatures. Determining where and when these different conditions apply could improve mechanistic understanding of malaria risk. More broadly, given that many aspects of ectotherm life history and fitness are characterized by non-linear thermal performance curves, we suggest that daily temperature dynamics could have marked effects on many species, affecting understanding of both current ecology and the expected responses to future climate change.

Results

Effects of environmental temperature on parasite development. We estimated the extrinsic incubation period of *Plasmodium falciparum* using long-term temperature data from four sites in Kenya: Kisumu, Garissa, Kitale and Kericho. Malaria transmission varies in both seasonality and intensity across these locations (e.g. see Refs. 11,12,22–27 and Table 1) with highest malaria incidence in Kisumu, followed by Kericho and Kitale[24]. Although Garissa has acute seasonal malaria transmission, parasite prevalence is low (<1% during the dry season)[23]. Even though malaria at these sites is variable, the sites were selected primarily to illustrate the contrasting thermal environments that can exist across relatively small spatial scales within a country. The sites are located at similar latitudes but vary in altitude (see Table 1) leading to marked differences in mean temperatures and diurnal temperature ranges (see Supplementary Fig. S1 online). Based on rate summation effects (discussed above), we expect these temperature differences to have divergent effects on parasite development (Figure 1). In Figure 1, the red line captures the full range of temperatures (minimum and maximum temperatures) at the field locations. Yellow circles represent the mean monthly temperature at each of the sites. Mean temperatures are coolest for Kericho (18°C) and Kitale (19°C), hottest for Garissa (29°C) and intermediate for Kisumu (24°C).

The effects of temperature on EIP were estimated using the thermodynamic parasite development model of Paaijmans *et al.*[15]. This model describes the rate of *Plasmodium falciparum* development across the parasite's operative temperature range (15.4 – 35.0°C – see Figure 1, Supplementary Fig. S1 online). EIP was estimated for each site using three measures of temperature derived from the climate data (see equations 1–7 in Table 2): (i) mean monthly temperature, (ii) mean daily temperature, and (iii) hourly temperatures (designated 'monthly', 'daily' and 'hourly' henceforth).

EIPs estimated using monthly, daily and hourly temperatures for each of the four sites are shown in Figure 2. For the warmest site (Garissa) the estimates of EIP based on mean monthly temperature and mean daily temperature were similar to one another, ranging from around 9–10.5 days (RMSE = 0.71). These EIPs were significantly shorter than the EIPs predicted using hourly temperatures, where parasite development was predicted to take between roughly 12–14 days ($\text{RMSE}_{\text{Daily vs Hourly}} = 2.41$; $\text{RMSE}_{\text{Monthly vs Hourly}} = 2.81$; $H(2) = 827.8$, $P < 0.001$).

Comparable patterns were also observed for the other 'warm' site, Kisumu. EIPs based on mean monthly temperature or mean daily temperatures were again similar, ranging from around 12.5–16.5 days across the year (RMSE = 0.57). The EIPs based on hourly temperatures were significantly longer, ranging from 15–18 days ($\text{RMSE}_{\text{Daily vs Hourly}} = 1.44$; $\text{RMSE}_{\text{Monthly vs Hourly}} = 1.76$; $H(2) = 269.5$, $P < 0.001$). Thus, in the warmer transmission environments, estimates of EIP increase as the resolution of the temperature data becomes more fine-scale. What we consider the 'true' EIP (i.e. based on the hour to hour fluctuations actually experienced by mosquitoes in the field) is longer than predicted from standard measures of environmental temperature such as daily or monthly means.

More marked but opposite patterns were revealed for the two 'cool' transmission sites. For Kericho, mean monthly and daily temperatures predicted similar parasite development (RMSE = 12.37), although because of the cooler temperatures, estimated EIPs were longer and more variable ranging from around 40–100 days (the temperature-growth relationship is strongly linear at lower temperatures so small changes in temperature have a greater effect on EIP). With hourly temperature data, estimated EIPs were greatly reduced ranging from 30–40 days ($\text{RMSE}_{\text{Daily vs Hourly}} = 22.8$; $\text{RMSE}_{\text{Monthly vs Hourly}} = 28.46$; $H(2) = 152.4$, $P < 0.001$).

For Kitale, EIPs based on mean monthly temperature or mean daily temperatures were again similar (23–50 days across the year, RMSE = 3.77). The EIPs based on hourly temperatures were significantly shorter, ranging from 23–35 days ($\text{RMSE}_{\text{Daily vs Hourly}} = 7.33$; $\text{RMSE}_{\text{Monthly vs Hourly}} = 7.81$; $H(2) = 67.3$, $P < 0.001$). Thus, in contrast to Kisumu and Garissa, in the cooler transmission environments, estimates of EIP decrease as the temporal resolution of the temperature data increases and the 'true' EIP is substantially shorter than predicted from daily or monthly means.

Country- and continent-wide implications. The preceding analysis indicates that estimates of parasite development rate differ depending on the temporal resolution of temperature data used

Table 1 | Summary data for the four study sites in Kenya. Data include elevation, meteorological station identifier, years of climate data used and climate summaries of each location. The sites exhibit a range of malaria parasite prevalence rates (*Plasmodium falciparum* prevalence rates, *pfpr*, extracted from the endemicity surface of transmission for 2007 (http://www.map.ox.ac.uk/data[12])

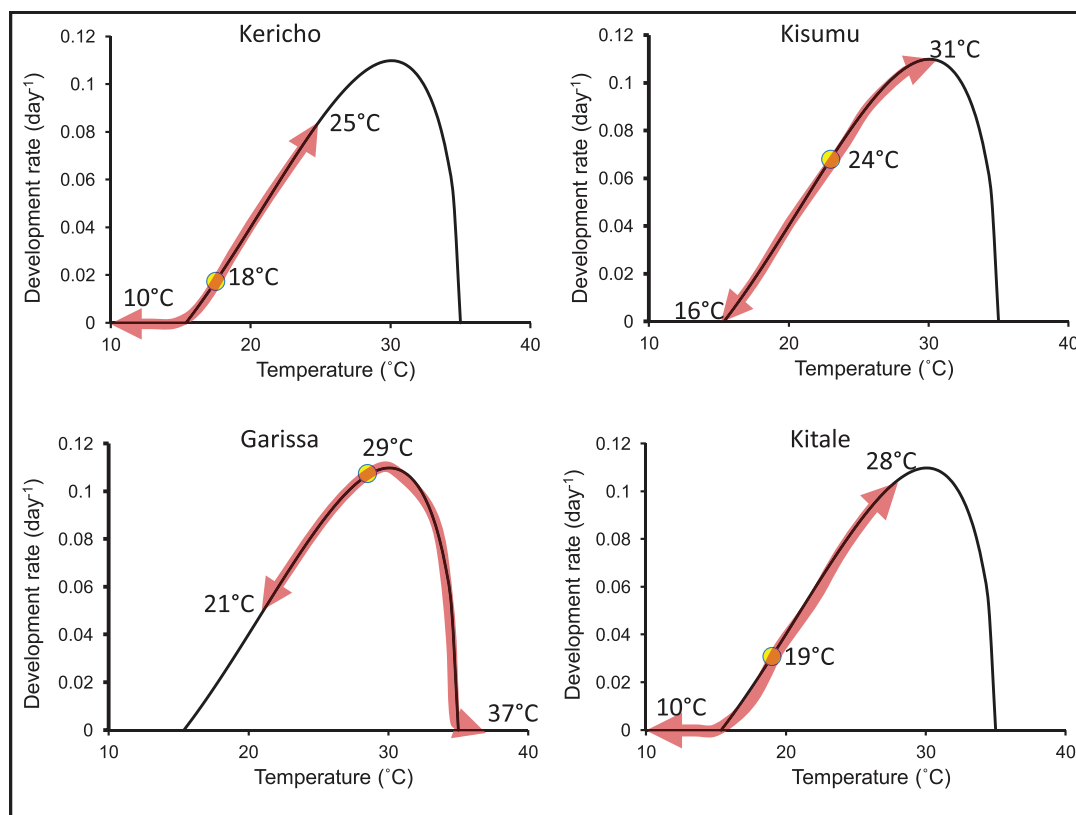| Station id	Station Name	Elevation (m)	Climate Data used	Plasmodium falciparum parasite prevalence rate (pfpr)	Climate Summary
637080	Kisumu	1146	1979–2009 (97.1% complete)	0.226	Annual Rainfall: 1311 mm Temperature: min: 16°C, max: 31°C DTR: 10–16°C
637100	Kericho	2184	1988–1997 (90.8% complete)	Epidemic or seasonal transmission; no endemic pfpr estimate available	Annual Rainfall: 1809 mm Temperature: min:10°C, max: 25°C DTR: 11–15°C
637230	Garissa	147	1981–2009 (96.7% complete)	0.017	Annual Rainfall: 431 mm Temperature: min: 21°C, max: 37°C DTR: 10–16°C
636610	Kitale	1875	1983–2004 (95.9% complete)	0.037	Annual Rainfall: 1172 mm Temperature: min: 10°C, max: 28°C DTR: 11–18°C

Figure 1 | Predicted thermal performance of malaria parasite development within the mosquito[15] in relation to the temperatures experienced at each of four study locations in Kenya, Africa.

(Figure 2). To estimate 'true' EIP we need to capture the influence of daily temperature fluctuations using hourly temperature data. Our four study sites were selected, in part, because of the availability of suitable temperature data. However, hourly temperature data do not exist for all locations in Kenya or across Africa. Accordingly, we approximated the average diurnal cycle for different locations by fitting a modified sine model[28] through mean monthly minimum and maximum temperature series based on 10 years of data (WorldClim by Hijmans, et al.[29]), to generate estimated hourly temperatures representative of a given month. We then used these monthly average diurnal cycle data to drive the thermodynamic model of EIP. Although, this method does not replicate precise diurnal temperature curves for each day, it does provide a measure of average diurnal fluctuation to compare to the single value of mean monthly temperature used in most other studies.

When we compared the monthly average diurnal cycle predictions of EIP with the monthly means of the 'true' EIPs derived from the hourly temperatures (averaged for each month) for the four locations in Kenya (Figure 3) we found that for three of the sites there were no significant differences between these different measures of EIP (Kisumu: $U = 68292.0$, $z = -0.31$, $P = 0.75$. Kericho: $U = 6506.0$, $z = -1.29$, $P = 0.12$. Kitale: $U = 32335.0$, $z = -1.43$, $P = 0.15$). There was a significant difference between the two approaches at the warmest site, Garissa ($U = 49841.0, z = -4.17, P < 0.001$). For this site the EIP estimates generated from the hourly temperatures were longer than those generated from the monthly max-min model. However, although statistically significant, the differences were extremely small (RMSE = 0.45 days). EIP from the hourly temperatures ranged from 10.2–14.4 days with a mean ($\pm$95% C.I.) of 11.9 $\pm$ 0.18 days, while EIP from the monthly diurnal model ranged from 10.2–14.1 days with a mean of 11.7 $\pm$ 0.19 days. Such small differences are unlikely to have any biological relevance. Thus, use of mean monthly maximum and minimum temperatures to generate an

average diurnal temperature profile yields robust estimates of the average of the 'true' EIPs exhibited across a month.

In Figure 4 we present maps of EIP for Kenya using one example month per quarter to represent variation across the year. We compare EIPs estimated using mean monthly temperatures (4A), with EIPs estimated using hourly temperatures from the average monthly diurnal temperature variation models (4B). Map 4C illustrates the percent change between A and B, with positive values (blue) indicating when B > A, and negative values (brown) when B < A. These maps support the patterns described above, whereby mean temperatures overestimate parasite development rate under warm conditions, provide a good approximation of growth under intermediate conditions, and underestimate development under cool conditions (Figure 4). For Kenya the most striking effects are in the highland areas to the west and north of Nairobi, where daily fluctuations in temperature suggest more extensive and more rapid (up to 100%) development than predicted using monthly mean temperatures. Constraining the EIP estimates to times where monthly rainfall >80 mm (this is a relatively conservative measure to describe the minimum rainfall required to support mosquito breeding – see methods) reduces the spatial distribution of potential malaria transmission but on the whole, does not lessen the relative differences between monthly and hourly predictions.

Scaling up further, we see considerable spatial and temporal variation in parasite development across Africa (Figure 5). As above, map 5A illustrates EIPs based on mean monthly temperatures. Map 5B illustrates EIPs based on an average diurnal cycle for the month and map 5C, the percent difference between 5A and 5B. Within large parts of central Africa in and around the equator, the estimates of EIP are similar between approaches indicating that mean monthly temperature is appropriate for characterizing the transmission environment. However, there are also many areas within the current malaria transmission range where mean monthly

Table 2 | Summary of data and models used to analyze change in the Extrinsic Incubation Period (EIP) (a) at each of the four sites in Kenya using monthly, daily and hourly scales (b) across Kenya and Africa based on monthly and hourly scales using a GIS and (c) the comparison of these outputs using the root mean square error

Temporal Scale	Data	Model	
(a) Site specific analysis			
Monthly	Mean monthly temperature (°C)	$r(T)_{EIPMonth} = 1/(0.000112T(T - 15.384)\sqrt{(35-T)})$	(1)
Daily	Daily mean temperature (°C)	$r(T)_{EIPDay} = (0.000112T(T - 15.384)\sqrt{(35-T)}$	(2)
	$Ta = (Tmax + Tmin)/2$	$s(rT_{EIPDay}) = \sum r(T^*)$	(3)
		where the daily rate of parasite development (rT^*) is estimated from the daily average temperature and accumulated over time until s (rT_{EIPDay}) = 1.	
Hourly	Hourly mean temperature (°C)	$r(T)_{EIPHour} = (0.000112T(T - 15.384)\sqrt{(35-T)})/24$	(4)
	Estimated from the daily maximum and minimum temperature using the Parton & Logan model[28]	$s(rT_{EIPHour}) = t \sum r(T^*)$	(5)
		where t = hourly time interval and the rate of parasite development (rT^*) is estimated from the average temperature occurring during hour (t) and accumulated over time until s (rT) = 1.	
		Parton & Logan model[28]:	
		$T_{day} = (T_{max} - T_{min}) \sin(\pi m/Y + 2a) + T_{min}$	(6)
		$T_{night} = T_{min} + (T_{sunset} - T_{min})\exp\text{-}(bn/Z)$	(7)
		T_{max} is daily maximum temperature (°C), T_{min} is daily minimum temperature (°C), T_{sunset} is the temperature recorded at sunset (°C), m is the number of hours after the occurrence of minimum temperature until sunset (h), n is the number of hours after sunset until the time of the minimum temperature (h), Z is the night length (h) and Y is the day length (h).	
		a = 1.5, b = 2.8 and c = −0.1	
(b) Geographic Information Systems (GIS)			
Monthly	Mean monthly temperature (°C) surfaces (WorldClim)	Same as equation 1	
		Indoor temperature was calculated as follows	
		$0.7717 T_{mean} + 6.9386$ ($R^2 = 0.80$) where T_{mean} is the mean monthly temperature (°C)	(8)
Hourly	Minimum mean monthly and maximum mean monthly temperature (°C) surfaces (WorldClim)	Same as equations 4, 5, 6, 7	
		Indoor temperatures were calculated as follows	
		$0.7801 T_{max} + 5.2677$ ($R^2 = 0.70$) where T_{max} is the monthly maximum temperature (°C);	(9)
		$0.6363 T_{min} + 9.8982$ ($R^2 = 0.76$) where T_{min} is the monthly minimum temperature (°C)	(10)
(c) Comparison of outputs			
RMSE	EIP values across the different temporal scales were compared by calculating the Root Mean Square Error (RMSE)	$RMSE = \sqrt{\sum (EIP\_x - EIP\_y)^2/N}$	(11)
		Where x and y are the different temperature scales (monthly, hourly, daily)	

temperatures under- or over- estimate EIP, sometimes by 100% or more. Again, adding the rainfall filter for mosquito breeding reduces the spatial distribution of potential malaria transmission but large differences between the monthly and hourly predictions remain. Given the sensitivity of malaria transmission to EIP (or more precisely the length of the EIP relative to daily mosquito survival[13]), such errors have important implications for understanding the spatial and temporal variation in malaria dynamics. For example, assuming a daily survival probability of adult mosquitoes of 0.86[5], a 5 day increase in EIP from a baseline value of 10 days would reduce the proportion of mosquitoes living long enough to transmit malaria from 0.221 to 0.104, which, assuming all else to be equal, would approximate a halving in transmission potential. Conversely, if conditions are cooler and the true EIP is predicted to be 30 days rather than 45 days, the proportion of mosquitoes living long enough to transmit malaria would increase from 0.001 to 0.011, representing an order of magnitude increase in transmission potential.

Thus far we have considered the influence of outdoor temperatures. This approach follows nearly every other malaria-temperature study published to date so is consistent with the 'industry standard'. However, adult mosquitoes can rest indoors (endophily) as well as outdoors (exophily), although there appears considerable variation between and within species (see later discussion). Data on the relationship between indoor and outdoor temperatures are extremely scant but to enable a preliminary investigation we apply simple regressions to predict indoor maximum and minimum temperatures based on published data from 8 locations in East Africa[30]. We use these regressions to generate maps of EIP corrected for indoor temperatures (Figure 6). We find that the general buffering nature of indoor environments reduces daily temperature variation and increases mean temperatures. Accordingly, the differences between predictions of EIP based on mean temperatures vs. hourly temperatures are reduced compared to the outdoor situation. However, the broad patterns are qualitatively similar (compare map 5C with 6C) and daily temperature variation still leads to percent differences in EIP of −100% to +77% relative to the monthly means. The differences are reduced slightly with the addition of the rainfall filter but still range between −50% to +50%.

Discussion

Our aim in the current study was to explore how different measures of environmental temperature influence estimates of the EIP. The current temperature-dependent models for the EIP of *P. falciparum*[1,15,31] draw heavily on limited empirical data from studies conducted on a Eurasian mosquito vector in the early part of last century[1,19]. EIPs from field infections have rarely been compared to model outputs. Given the significance of EIP in determining transmission intensity and how widely the standard degree-day model of
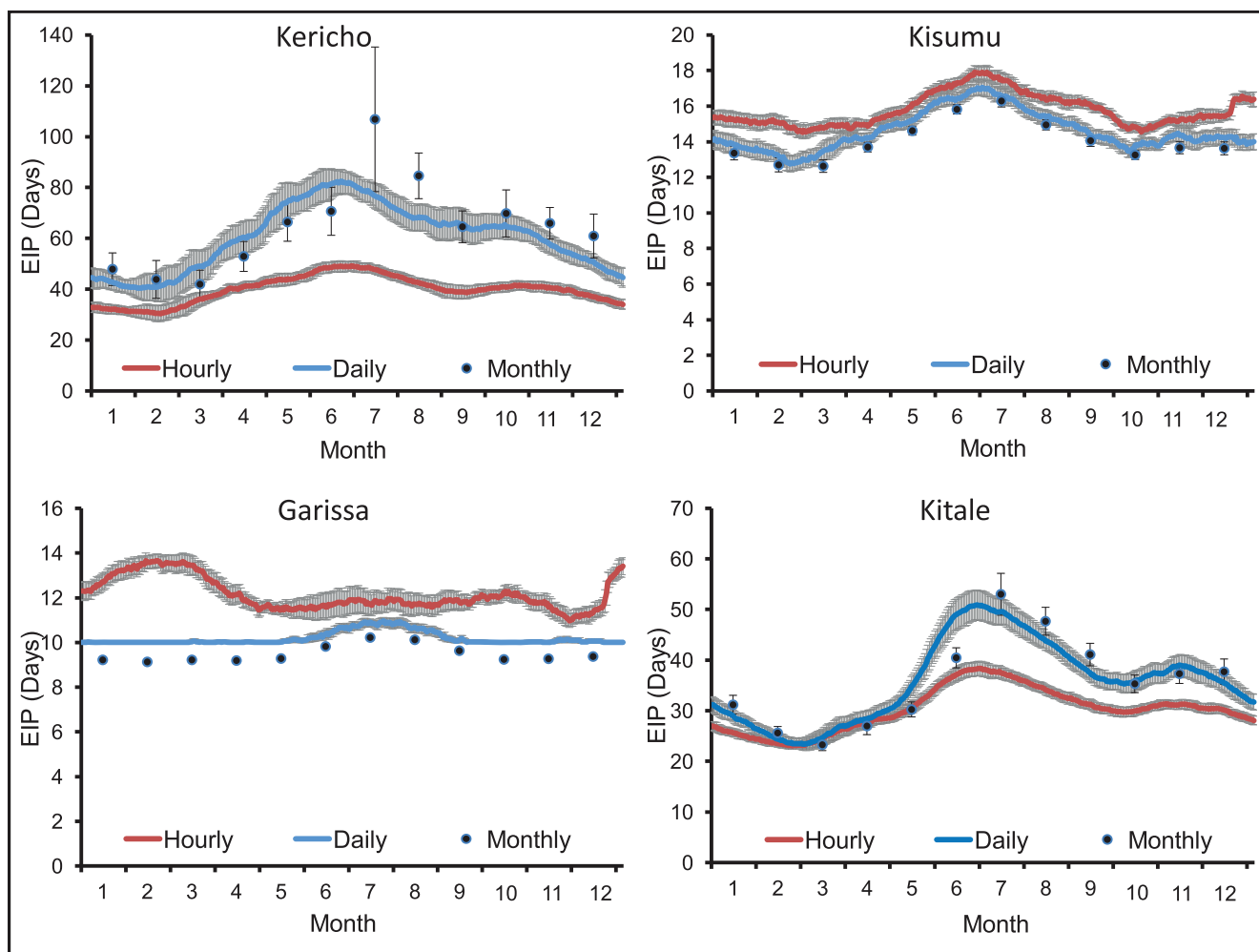
Figure 2 | Estimated mean (±95% C.I.) Extrinsic Incubation Period (EIP) (days) of *P. falciparum* for four locations in Kenya, calculated using monthly, daily or hourly temperatures. Details of temperature time series given in Table 1.

Detinova[1] has been applied, it is surprising how little work has been done to validate this relationship and to quantify whether, for example, the temperature-dependence of *P. falciparum* (or *P. vivax*) is consistent across different mosquito species and/or parasite clones.

These issues notwithstanding, we find that estimates of EIP depend strongly on the temporal resolution of the temperature data used to drive the parasite development model. Under cool conditions (and especially with large diurnal temperature ranges) the use of standard metrics such as mean monthly temperatures will tend to underestimate parasite development. This effect is nicely illustrated for Kericho in the Kenyan highlands where EIPs predicted using mean daily or monthly temperatures frequently exceed the maximum predicted lifespan of the mosquito vectors (56 days, see Ref. 3), including during the known peak malaria season (March-July). In contrast, under warmer conditions, use of mean temperatures alone will over-estimate parasite development. Thus, in areas of the Sahel and also Garissa, our warmest site in Kenya, we predict the true EIP to be longer than predicted using mean temperatures. At intermediate temperatures, such as in the thermally stable lowland environments around the equator, mean temperatures appear to provide a good approximation of the thermal environment. Kisumu in western Kenya is representative of this situation, with very small differences between the different estimates of EIP.

The EIP is only one parameter determining transmission intensity and so the results presented here are not intended to provide quantitative measures of malaria transmission risk. In different areas malaria might be constrained by many factors including low humidity[32], lack of water for breeding sites[32,33] or by human activities[34], irrespective of EIP. Indeed, when we add a constraint for the minimum rainfall necessary for mosquito breeding, we find that the spatial extent of potential malaria transmission in any one period is reduced. However, the importance of daily temperature variation remains. Other studies have considered a broader set of both biological and environmental parameters to determine malaria transmission intensity[3,11–13]. This research includes some influential malaria mapping work to inform contemporary public health strategies[12,35,36]. Yet no studies have explored the influence of daily temperature variation in the way we consider here. Use of simple degree-day models that consider only the linear parts of a thermal performance curve will tend not to capture the full effects of daily temperature dynamics (e.g. see Refs. 7,11).

Individual mosquito species tend to exhibit different extents of endophily vs. exophily and while there are some generalizations, resting behaviour appears to be relatively plastic[30]. Indeed, some studies report no significant tendency for repeated endophily or exophily for even the same individual mosquito[37,38]. Moreover, there is evidence that current vector control tools such as indoor residual insecticide sprays and insecticide treated nets are selecting for outdoor biting and resting[39–41]. Thus, characterizing the effects of outdoor temperatures is clearly relevant to malaria transmission ecology. That said, indoor resting is also important yet virtually no studies have considered indoor temperatures (see Refs. 30,42 for
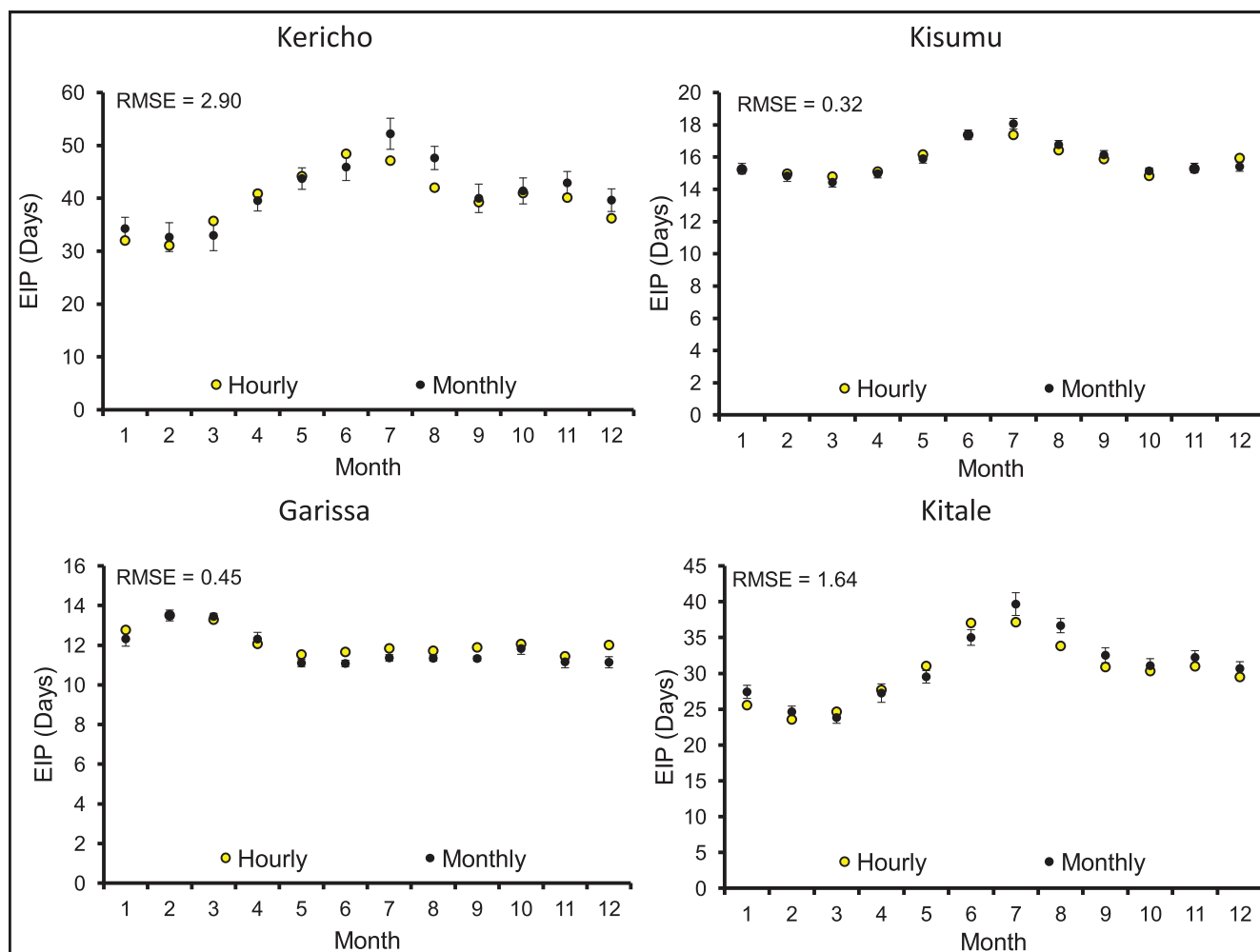
5

Figure 3 | Comparison of mean (±95% C.I.) Extrinsic Incubation Periods (EIP) for four sites in Kenya calculated using a diurnal temperature cycle model based on monthly maximum and minimum temperatures ('Monthly' EIPs - black symbols) or the hourly temperatures for the equivalent months (Hourly EIPs - yellow symbols).

exceptions). The data on indoor temperatures are extremely limited and the conditions themselves are expected to vary considerably depending on house design, construction materials, housing density, adjacent vegetation cover and altitude[30,42]. Given the limited nature of the data, the regressions we apply to predict indoor temperatures based on outdoors should be treated with some caution. Nonetheless, our analysis suggests that while indoor environments are relatively thermally buffered, daily temperature variation still matters.

More broadly, our analysis of EIP illustrates the effects of temperature on a life history trait characterized by a non-linear, asymmetric thermodynamic curve. Several of the other mosquito traits that contribute directly or indirectly to malaria transmission intensity (e.g. fecundity, duration of gonotrophic cycle, larval development rate), follow this general pattern[3,4,43]. Such curves have also been widely used to describe the thermal performance of other taxa, considering both individual life history traits and composite fitness metrics such as intrinsic rate of increase (r) and basic reproductive numbers (R_o)[44–47]. Thermal performance curves tend to be derived from constant temperature experiments conducted under controlled laboratory conditions (e.g. see the majority of species listed in[46]). As with the EIP, integrating the effects of daily variation around mean temperatures will likely alter estimates of performance over both time and space; we suggest that the qualitative patterns we have revealed will apply to multiple traits across diverse systems.

Numerous studies provide evidence that short-term environmental variation has the potential to affect life history traits and

fitness above and beyond the effects of mean temperatures alone (e.g. Refs. 14,16,18,48–52). Yet other studies highlight the importance of temperature fluctuations for acclimation and adaptation[53,54] and in the evolution of thermal optima[55,56]. However, in spite of this research, the vast majority of ecological studies examining temperature-dependent effects consider mean temperatures alone. Incorporating the effects of daily temperature variation could improve mechanistic understanding of ectotherm ecology, and provide new insights into likely impacts of anthropogenic climate change on pest and disease risk[20,50,57], species range expansions and contractions[58,59], and biodiversity loss[53,60].

Methods

Environmental characteristics. Daily minimum and maximum temperature data for each of the four sites in Kenya were obtained from the Global Surface Summary of the Day Database (Version 7), National Climate Data Center website (http://www.ncdc.noaa.gov/) (GSOD NOAA). Consecutive years with the least number of missing days were selected to represent each station (Table 1). Missing temperature values were infilled using temperature averages based on the 15 days preceding and 15 days following the missing date across all the years in the data set. These long-term temperature data were used to estimate extrinsic incubation period of *Plasmodium falciparum* from four sites in Kenya: Kisumu, Garissa, Kitale and Kericho.

Quantifying the effects of environmental temperature on parasite development. The rate of parasite development across a range of temperatures was estimated by the model of Paaijmans *et al.*[15]. This model was used to estimate the effects of monthly, daily and hourly temperatures on EIP for each site (see equations 1–7 in Table 2). The model largely follows the widely used degree-day model for malaria parasite
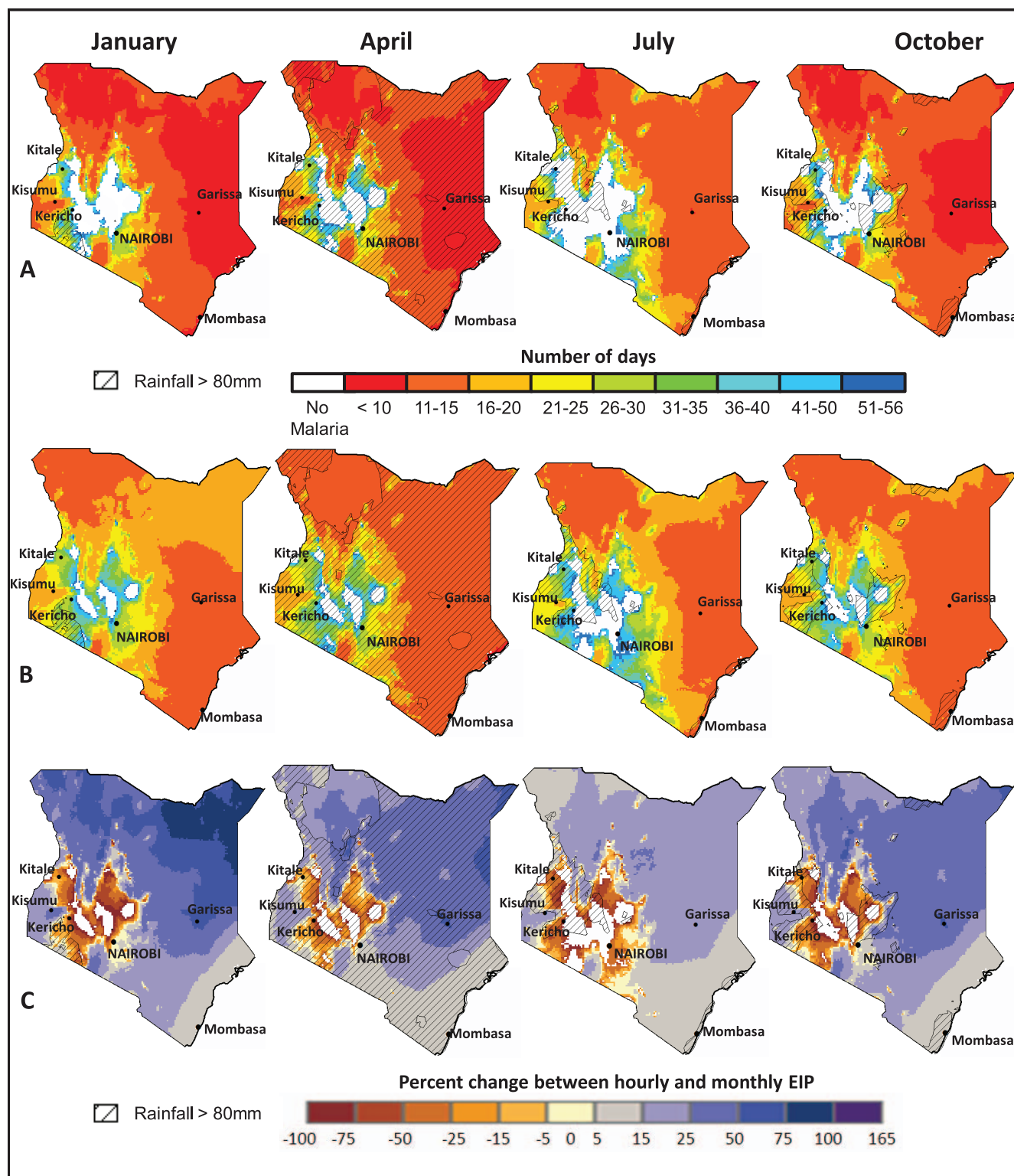
Figure 4 | Maps illustrating number of days for malaria to become transmittable (EIP) across Kenya. Map **A** illustrates the number of days taken to complete EIP using mean monthly temperatures. Map **B** illustrates the number of days taken to complete EIP using hourly temperatures based on an average diurnal cycle for the month. Map **C** illustrates the percent change between **A** and **B**. Positive values (blue) show when EIP values for **B** are greater than EIP values for **A**, and negative values (brown) show when EIP values for **B** are less than EIP values for **A**. Hatched areas indicate where sufficient rainfall (> 80 mm) has fallen to support mosquito breeding.

development of Detinova[1] but allows for the effect of temperature fluctuations that extend beyond the linear part of the thermal performance curve. Where temperatures fell outside the operative range, development was set to zero. For each of these estimates, growth rates from the temperature-dependent model were accumulated using the respective temperature measures until they reached a value of 1, which

defines the completion of the extrinsic incubation period. For the 'hourly' estimates we fitted a modified sine model[28] to interpolate between the daily maximum and minimum temperatures and accumulated development rate at hourly intervals. An upper threshold for the EIP duration was set to 56 days, the upper limit of mosquito longevity used in a number of previous studies[3,15]. The data and models used to
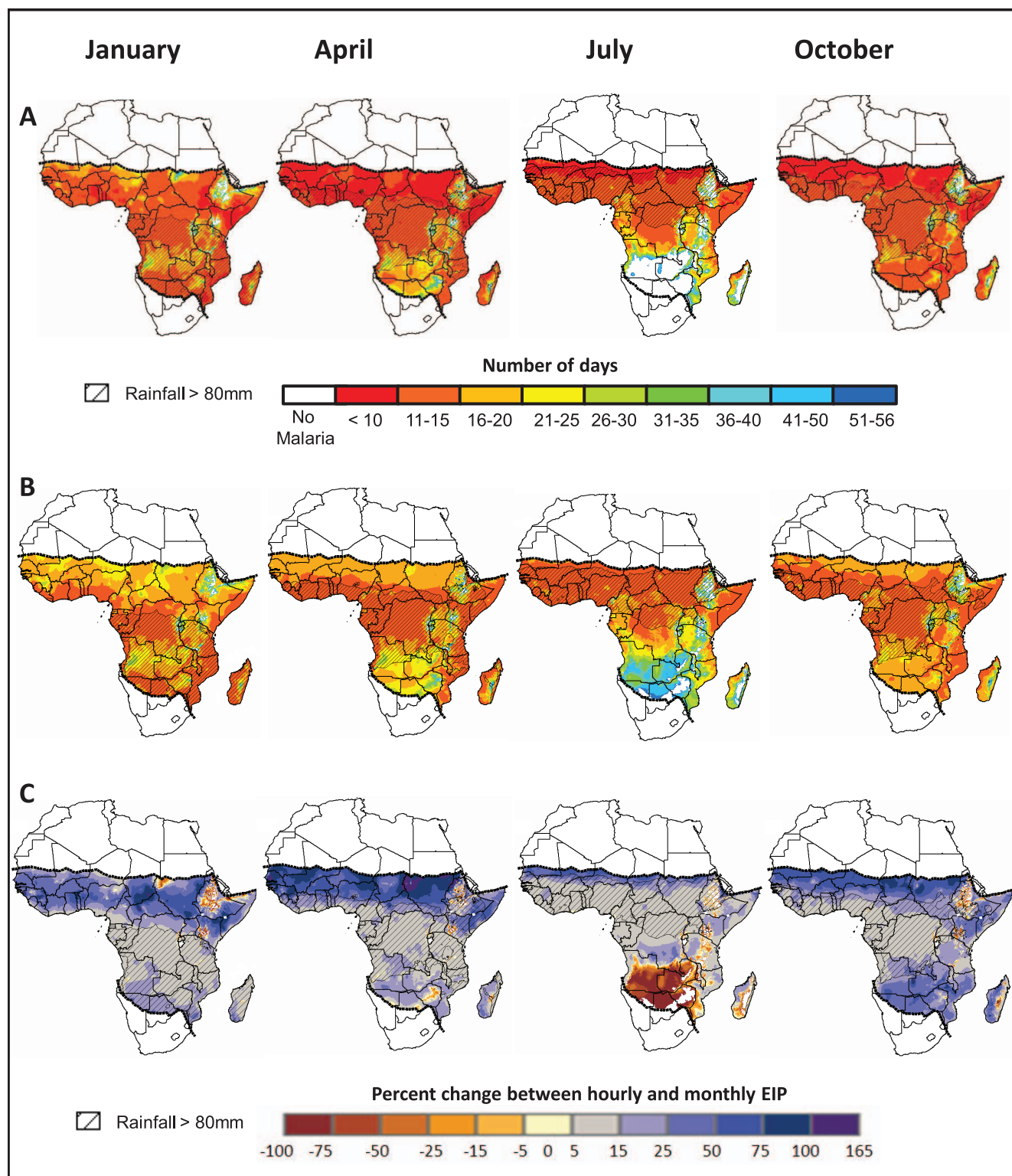
Figure 5 | Maps illustrating number of days for malaria to become transmittable across Africa within the defined malaria transmission zone utilizing outdoor temperature. Maps A, B and C as in Figure 4.

perform these assessments are summarized in Table 2. Thus, monthly EIP was calculated using a single mean monthly temperature value; daily EIP was calculated for each day of the year using the daily mean temperature; hourly EIP was calculated for each hour of each day of the year using the hourly mean temperature.

Initial comparisons between EIP estimates at the different temporal scales were made by calculating the root mean square error. The root mean squared error (RMSE)-- the square root of the variance of the difference plus the square of the mean (Eq. 11, Table 2)-- is an absolute indication of the difference between measurement

scales. The lower the RMSE value, the less difference in EIP and the larger value, the greater the difference. In addition we tested our results to see if differences in EIP were significant. EIP measurement variance was not homogenous and could not be transformed to meet Gaussian assumptions, hence non-parametric tests were used. A Kruskal-Wallis test using Monte Carlo methods was used for comparing the monthly, daily and hourly estimates for each site. Subsequently tests between measurement levels were conducted using Mann-Whitney tests again using the Monte Carlo method. Because of the danger of inflating the Type 1 error rate, a Bonferroni
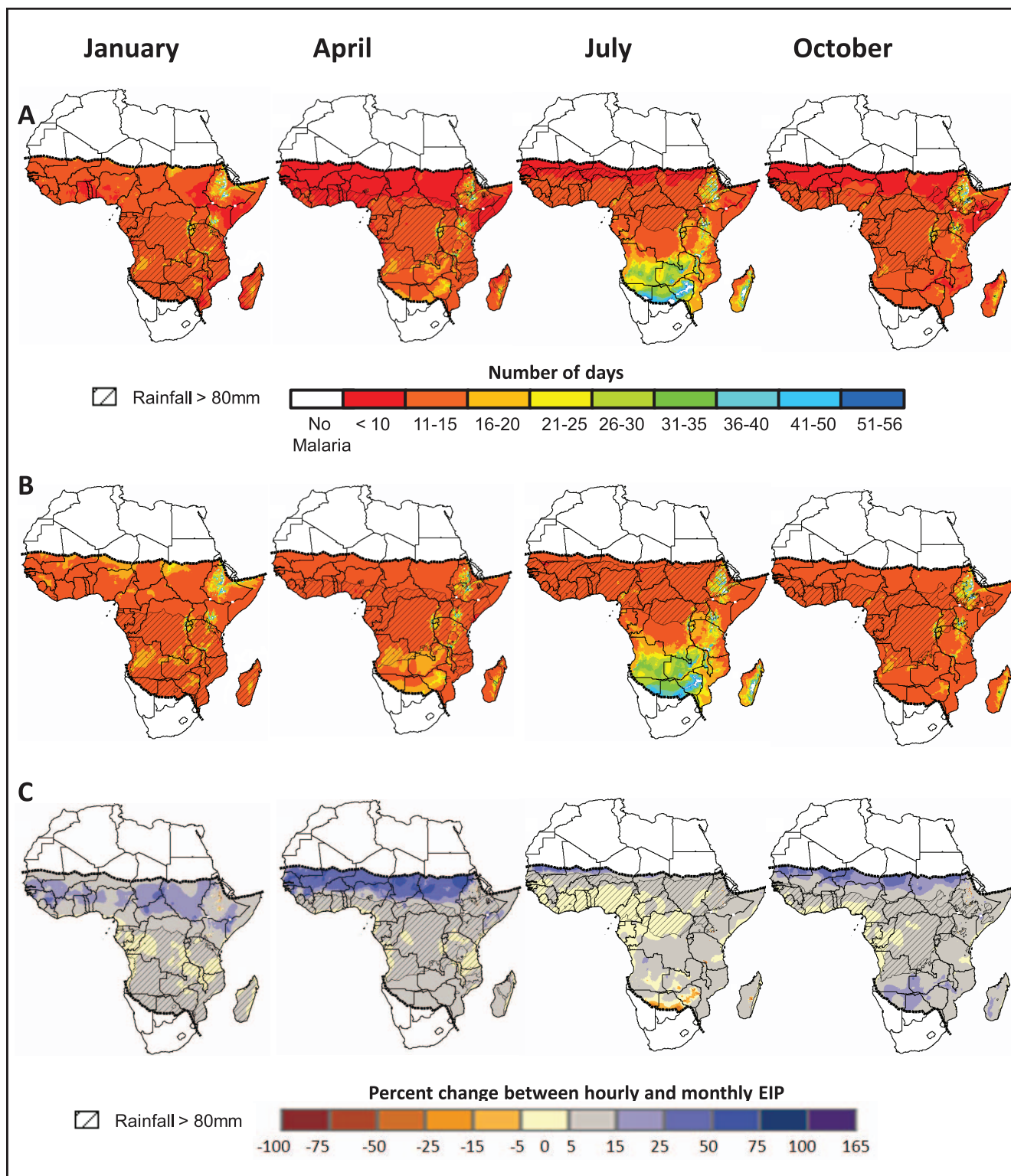
Figure 6 | Maps illustrating number of days for malaria to become transmittable across Africa within the defined malaria transmission zone using indoor temperature. Maps A, B and C as in Figure 4.

correction was applied and all effects are reported at the 0.0167 level of significance for these *post hoc* tests.

Mapping EIP across Africa. To conduct the broad-scale spatial analyses we integrated the parasite development model into a Geographic Information System (GIS) (equations in Table 2). Minimum and maximum mean monthly temperature surfaces were created using thinplate smoothing spline interpolation method and obtained from WorldClim, version 1.4 (release 3) (http://www.worldclim.org29). These surfaces were imported into ESRI™ ArcGIS ArcView 10 and integrated with

the Paaijmans *et al.*[15] model to create monthly and hourly EIP maps for Africa. Monthly estimates were created using equation 1 (Table 2) and hourly estimates were made using equation 4–7 (Table 2).

Numerous malaria-modeling studies have utilized WorldClim data (e.g. Refs. 6,7,47). As partial validation of these data, we compared the GSOD NOAA monthly temperature values (estimated from the daily temperature data values) with the WorldClim monthly values used to generate the temperature surfaces for each of the four sites in Kenya. This analysis revealed Root Mean Square Errors ranging from 0.33–1.98 for all paired comparisons of minimum, maximum and

mean monthly temperature for each site. Root Mean Square Errors were smallest for mean monthly temperature (0.33 (Kitale), 0.47 (Kisumu) and 0.51 (Garissa and Kericho)) with greater differences occurring between sites for minimum temperatures (0.44 (Garissa), 1.0 (Kisumu), 1.97 (Kericho) and 1.98 (Kitale)) and maximum temperature (0.68 (Kisumu), 1.15 (Kericho), 1.36 (Garissa) and 1.59 (Kitale)).

Indoor temperature estimates were determined using the regression equations (Eq. 8, 9 and 10) in Table 2 that capture the relationship between indoor and outdoor temperatures at different elevations[30]. These regressions were used to convert the outdoor temperature surfaces to matching estimates of indoor temperatures. We then applied appropriate equations from Table 2 to generate estimates of EIP based on indoor monthly mean temperatures and the average daily temperature range.

Limits of *Plasmodium falciparum* malaria transmission zones were obtained from the 2007 malaria map of Africa from the malaria atlas project (http://www.map.ox.ac.uk/data12). An image of the map was brought into ArcGIS ArcView 10, geo-referenced and the malaria transmission limits were digitized. The limits were used to constrain our mapped outputs to the existing malaria transmission boundaries. We add a further possible filter on transmission by highlighting (hatched shading) areas that received greater than 80 mm of rainfall on average during the time period shown. This level of rainfall has been used elsewhere to indicate conditions suitable for mosquito breeding (see Ref. 3), although it ignores the influence of permanent water bodies, dams, wells, irrigated areas, water storage containers etc. that can sustain mosquito populations under reduced rainfall conditions[61]. Monthly rainfall data were obtained from WorldClim.

1. Detinova, T. S. Age-grouping methods in Diptera of medical importance with special reference to some vectors of malaria. *Monograph Series. World Health Organization* **47**, 13–191 (1962).
2. Noden, B. H., Kent, M. D. & Beier, J. C. The impact of variations in temperature on early *Plasmodium falciparum* development in *Anopheles stephensi*. *Parasitology* **111**, 539–545 (1995).
3. Craig, M. H., Snow, R. W. & le Sueur, D. A climate-based distribution model of malaria transmission in sub-Saharan Africa. *Parasitol Today* **15**, 105–111 (1999).
4. Bayoh, M. N. & Lindsay, S. W. Effect of temperature on the development of the aquatic stages of *Anopheles gambiae* sensu stricto (Diptera: Culicidae). *Bulletin of Entomological Research* **93**, 375–381 (2003).
5. Kiszewski, A. *et al.* A global index representing the stability of malaria transmission. *Am J Trop Med Hyg* **70**, 486–498 (2004).
6. Guerra, C. A. *et al.* The limits and intensity of *Plasmodium falciparum* transmission: Implications for malaria control and elimination worldwide. *Plos Medicine* **5**, 300–311 (2008).
7. Gething, P. W. *et al.* Modelling the global constraints of temperature on transmission of *Plasmodium falciparum* and *P. vivax*. *Parasite & Vector* **4** (2011).
8. Grover-Kopec, E. *et al.* An online operational rainfall-monitoring resource for epidemic malaria early warning systems in Africa. *Malaria J* **4** (2005).
9. Thomson, M. C., Mason, S. J., Phindela, T. & Connor, S. J. Use of rainfall and sea surface temperature monitoring for malaria early warning in Botswana. *Am J Trop Med Hyg* **73**, 214–221 (2005).
10. Mordecai, E. A. *et al.* Optimal temperature for malaria transmission is dramatically lower than previously predicted. *Ecology letters* **16**, 22–30 (2013).
11. Gething, P. W. *et al.* A new world malaria map: *Plasmodium falciparum* endemicity in 2010. *Malaria J* **10**, 378 (2011).
12. Hay, S. I. *et al.* A world malaria map: *Plasmodium falciparum* endemicity in 2007. *PLOS Medicine* **6** (2009).
13. Lindsay, S. W. & Martens, W. J. M. Malaria in the African highlands: past, present and future. *Bull WHO* **76**, 33–45 (1998).
14. Paaijmans, K. P. *et al.* Influence of climate on malaria transmission depends on daily temperature variation. *P Natl Acad Sci USA* **107**, 15135–15139 (2010).
15. Paaijmans, K. P., Read, A. F. & Thomas, M. B. Understanding the link between malaria risk and climate. *P Natl Acad Sci USA* **106**, 13844–13849 (2009).
16. Lambrechts, L. *et al.* Impact of daily temperature fluctuations on dengue virus transmission by *Aedes aegypti*. *P Natl Acad Sci USA* **108**, 7460–7465 (2011).
17. Ruel, J. J. & Ayres, M. P. Jensen's inequality predicts effects of environmental variation. *Trends Ecol Evol* **14**, 361–366 (1999).
18. Martin, T. L. & Huey, R. B. Why "suboptimal" is optimal: Jensen's inequality and ectotherm thermal preferences. *Am. Nat.* **171**, E102–118 (2008).
19. Macdonald, G. *The epidemiology and control of Malaria.* (Oxford University Press, 1957).
20. Rogers, D. J. & Randolph, S. E. in Advances in Parasitology, Vol 62: Global Mapping of Infectious Diseases: Methods, Examples and Emerging Applications. Vol. 62, *Advances in Parasitology* (eds Hay, S. I., Graham, A. & Rogers, D. J.) 345–381 (2006).
21. Smith, D. L. *et al.* Ross, Macdonald, and a theory for the dynamics and control of mosquito-transmitted pathogens. *PLoS pathog* **8** (2012).
22. Githeko, A. K. *et al.* Some observations on the biting behavior of *Anopheles gambiae* s.s., *Anopheles arabiensis*, and *Anopheles funestus* and their implications for malaria control. *Exp Parasitol* **82**, 306–315 (1996).
23. Lawford, H. *et al.* Adherence to prescribed artemisinin-based combination therapy in Garissa and Bunyala districts, Kenya. *Malaria J* **10**, 281(2011).
24. Okiro, E. *et al.* Malaria paediatric hospitalization between 1999 and 2008 across Kenya. *BMC Med* **18**, (2009).
25. Noor, A. M. *et al.* The risks of malaria infection in Kenya in 2009. *BMC Inf Dis* **9**, (2009).
26. Shanks, G. D., Hay, S. I., Omumbo, J. A. & Snow, R. W. Malaria in Kenya's western highlands. *Emerg Infect Dis* **11**, 1425–1432 (2005).
27. Snow, R. W. *et al.* The coverage and impact of malaria intervention in Kenya 2007–2009. *Division of Malaria Control, Ministry of Public Health and Sanitation, December 2009 (2009)* <http://www.map.ox.ac.uk/client_media/publications/DOMC_ME_report_2007-09_281109.pdf>. Accessed Dec 18th 2011.
28. Parton, W. J. & Logan, J. A. A model for diurnal-variation in soil and air-temperature. *Agr Meteorol* **23**, 205–216 (1981).
29. Hijmans, R. J., Cameron, S. E., Parra, J. L., Jones, P. G. & Jarvis, A. Very high resolution interpolated climate surfaces for global land areas. *Int J Climatol* **25** (2005).
30. Paaijmans, K. P. & Thomas, M. B. The influence of mosquito resting behaviour and associated microclimate for malaria risk. *Malaria J* **10**, 183 (2011).
31. Ikemoto, T. Tropical malaria does not mean hot environments. *J. Med. Entomol.* **45**, 963–969 (2008).
32. Gray, E. M. & Bradley, T. J. Physiology of desiccation resistance in *Anopheles gambiae* and *Anopheles arabiensis*. *Am J Trop Med Hyg* **73**, 553–559 (2005).
33. Shililu, J. I. *et al.* Development and survival of *Anopheles gambiae* eggs in drying soil: influence of the rate of drying, egg age, and soil type. *J Am Mosquit Contr* **20**, 243–247 (2004).
34. Gething, P. W., Patil, A. P. & Hay, S. I. Quantifying aggregated uncertainty in *Plasmodium falciparum* malaria prevalence and populations at risk via efficient space-time geostatistical joint simulation. *PLoS Comp Biol* **6**, e1000724 (2010).
35. Smith, D. L., Smith, T. A. & Hay, S. I. in *In Shrinking the Malaria Map: a Prospectus on Malaria Elimination* (ed Feachem, R. G. A., Phillips, A. A. and Targett, G. A. on behalf of the Malaria Elimination Group) 108–126. (The Global Health Group, University of California, San Francisco: San Francisco, U.S.A., 2009).
36. White, M. T. *et al.* Modelling the impact of vector control interventions on *Anopheles gambiae* population dynamics. *Parasit Vectors* **4**, 153 (2011).
37. Githeko, A. K., Service, M. W., Mbogo, C. M. & Atieli, F. K. Resting behaviour, ecology and genetics of malaria vectors in large scale agricultural areas of Western Kenya. *Parassitologia* **38**, 481–489 (1996).
38. Lines, J. D., Lyimo, E. O. & Curtis, C. F. Mixing of indoor-resting and outdoor-resting adults of *Anopheles gambiae* Giles S. L. and *Anopheles funestus* Giles (Diptera, Culicidae) in Coastal Tanzania. *Bulletin of Entomological Research* **76**, 171–178 (1986).
39. Reddy, M. R. *et al.* Outdoor host seeking behaviour of *Anopheles gambiae* mosquitoes following initiation of malaria vector control on Bioko Island, Equatorial Guinea. *Malaria J* **10**, 184 (2011).
40. Stevenson, J. *et al.* Novel vectors of malaria parasites in the Western highlands of Kenya. *Emerg Infect Dis* **18**, 1547–1549 (2012).
41. Bayoh, M. N. *et al. Anopheles gambiae*: historical population decline associated with regional distribution of insecticide-treated bed nets in western Nyanza Province, Kenya. *Malaria J* **9**, 62 (2010).
42. Alonso, D., Bouma, M. J. & Pascual, M. Epidemic malaria and warmer temperatures in recent decades in an East African highland. *Proc R Soc B* **278**, 1661–1669 (2011).
43. Lardeux, F. J., Tejerina, R. H., Quispe, V. & Chavez, T. K. A physiological time analysis of the duration of the gonotrophic cycle of *Anopheles pseudopunctipennis* and its implications for malaria transmission in Bolivia. *Malaria J* **7** (2008).
44. Briere, J. F., Pracros, P., Le Roux, A. Y. & Pierre, J. S. A novel rate model of temperature-dependent development for arthropods. *Environ. Entomol.* **28**, 22–29 (1999).
45. Clusella-Trullas, S., Blackburn, T. M. & Chown, S. L. Climatic predictors of temperature performance curve parameters in ectotherms imply complex responses to climate change. *Am. Nat.* **177**, 738–751(2011).
46. Deutsch, C. A. *et al.* Impacts of climate warming on terrestrial ectotherms across latitude. *P Natl Acad Sci USA* **105**, 6668–6672 (2008).
47. Parham, P. E. & Michael, E. Modelling climate change and malaria transmission. *Adv Exp Med Biol* **673**, 184–199 (2010).
48. Duncan, A. B., Fellous, S. & Kaltz, O. Temporal variation in temperature determines disease spread and maintenance in *Paramecium microcosm* populations. *Proc R Soc B* **278**, 3412–3420 (2011).
49. Klass, J. I., Blanford, S. & Thomas, M. B. Development of a model for evaluating the effects of environmental temperature and thermal behaviour on biological control of locusts and grasshoppers using pathogens. *Agr Forest Entomol* **9**, 189–199 (2007).
50. Rohr, J. R. *et al.* Frontiers in climate change-disease research. *Trends Ecol Evo* **26**, 270–277 (2011).
51. Liu, S. S., Zhang, G. M. & Zhu, J. Influence of temperature-variations on rate of development in insects - analysis of case-studies from entomological literature. *Ann Entomol Soc Am* **88**, 107–119 (1995).
52. Bozinovic, F. *et al.* The mean and variance of environmental temperature interact to determine physiological tolerance and fitness. *Physiol Biochem Zool* **84**, 543–552 (2011).
53. Dillon, M. E., Wang, G., Garrity, P. A. & Huey, R. B. Thermal preference in *Drosophila*. *J Therm Biol* **34**, 109–119 (2009).

54. Rohr, J. R. & Raffel, T. R. Linking global climate and temperature variability to widespread amphibian declines putatively caused by disease. *P Natl Acad Sci USA* **107**, 8269–8274 (2010).

55. Asbury, D. A. & Angilletta, M. J. Thermodynamic eEffects on the evolution of performance curves. *Am. Nat.* **176**, E40–E49 (2010).

56. Frazier, M. R., Huey, R. B. & Berrigan, D. Thermodynamics constrains the evolution of insect population growth rates: "Warmer is better". *Am Nat* **168**, 512–520 (2006).

57. Dangles, O., Carpio, C., Barragan, A. R., Zeddam, J. L. & Silvain, J. F. Temperature as a key driver of ecological sorting among invasive pest species in the tropical Andes. *Ecol Appl* **18**, 1795–1809 (2008).

58. Chen, I. C., Hill, J. K., Ohlemuller, R., Roy, D. B. & Thomas, C. D. Rapid range shifts of species associated with high levels of climate warming. *Science* **333**, 1024–1026 (2011).

59. Pateman, R. M., Hill, J. K., Roy, D. B., Fox, R. & Thomas, C. D. Temperature-dependent alterations in host use drive rapid range expansion in a butterfly. *Science* **336**, 1028–1030 (2012).

60. Thomas, C. D. *et al.* Extinction risk from climate change. *Med Vet Entomol* **427**, 145–148 (2004).

61. Walker, K. & Lynch, M. Contributions of *Anopheles* larval control to malaria suppression in tropical Africa: review of achievements and potential. *Med Vet Entomol* **21**, 2–21 (2007).

Acknowledgments

Author contributions

Conceived and designed paper: M.B.T., K.P.P., R.G.C., M.E.M., S.B., J.I.B. Data Analysis: J.I.B., S.B., K.V.S. Wrote the paper: M.B.T. and J.I.B., with additional input from S.B., K.V.S. All authors commented on and approved the final version of the manuscript.

Additional information

How to cite this article: Blanford, J.I. *et al.* Implications of temperature variation for malaria parasite development across Africa. *Sci. Rep.* **3**, 1300; DOI:10.1038/srep01300 (2013).